



MIT Open Access Articles

EXPERIMENTAL INVESTIGATION OF HIGH EFFICIENCY SINGLE-STAGE MEMBRANE DISTILLATION CONFIGURATIONS

The MIT Faculty has made this article openly available. **Please share** how this access benefits you. Your story matters.

Citation	Swaminathan, Jaichander, Hyung Won Chung, David M. Warsinger, and John H. Lienhard V. "EXPERIMENTAL INVESTIGATION OF HIGH EFFICIENCY SINGLE-STAGE MEMBRANE DISTILLATION CONFIGURATIONS." 2015 International Desalination Association World Congress on Desalination and Water Reuse (September 2015).
As Published	http://s23.a2zinc.net/clients/IDA/IDAWC15/Public/SpeakerDetails.aspx?FromPage=Speakers.aspx&ContactID=263
Publisher	International Desalination Association
Version	Author's final manuscript
Accessed	Thu Jan 17 16:43:45 EST 2019
Citable Link	http://hdl.handle.net/1721.1/100446
Terms of Use	Creative Commons Attribution-Noncommercial-Share Alike
Detailed Terms	http://creativecommons.org/licenses/by-nc-sa/4.0/

EXPERIMENTAL INVESTIGATION OF HIGH EFFICIENCY SINGLE-STAGE MEMBRANE DISTILLATION CONFIGURATIONS

Authors: Jaichander Swaminathan, Hyung Won Chung, David M. Warsinger, John H. Lienhard V

Presenter: Jaichander Swaminathan
Doctoral Candidate and Research Assistant, Mechanical Engineering Department,
Massachusetts Institute of Technology, Cambridge, MA 02139, USA

Abstract

A novel single-stage membrane distillation (MD) configuration, known as conductive gap membrane distillation (CGMD), has been suggested by numerical modeling results to achieve up to two times higher energy efficiencies than conventional air gap MD systems. CGMD consists of an MD module with a high thermal conductivity material in the gap region between the membrane and condensing plate, increasing the effective thermal conductivity of the gap. Such systems, if realized practically, could make MD competitive as a large scale thermal desalination technology that is not restricted only to specialized waste heat applications and could also make a stronger case for MD's use in waste-heat applications. In this study, an experimental comparison of different MD configurations is carried out on a bench scale system keeping membrane area constant, and results are compared to model predictions. The role of energy recovery within the module on improving CGMD efficiency is illustrated. A system with a simple copper woven mesh introduced in the gap in the place of plastic spacers is found to have 40% to 60% higher GOR than AGMD. The potential for further improvements in GOR and issues associated with studying MD efficiency at a laboratory bench scale are also discussed.



I. INTRODUCTION

Membrane distillation (MD) systems have been proposed for scalable desalination of a wide range of feed solutions. In terms of energy efficiency, the MD system's performance has been rated over a wide range of values [1, 2]. GOR values for real MD systems have typically been 2 to 4 [3, 4], while theoretical analysis has predicted numbers higher than 10 for several stacked configurations [5, 6]. If in reality a GOR close to 10 can be achieved with MD, the technology can potentially compete with other larger scale systems of similar energy efficiency such as MVC, MED, and MSF, due to MD's potentially lower capital expenditure and simpler system design.

Several configurations of MD have been proposed in the literature, including direct contact MD (DCMD), Sweeping Gas MD (SGMD), Air Gap MD (AGMD), Vacuum MD (VMD), and Permeate Gap MD (PGMD). Previous work by Summers et al. [7] has shown that single stage VMD has GOR values are below 1. Similar results were obtained by Swaminathan and Lienhard [8][8] for single stage sweeping gas MD (SGMD) systems, where the maximum GOR was below 3. Among other MD configurations, no clear ranking has been established.

Permeate Gap MD has been proposed and implemented as a modification of DCMD enabling direct energy recovery within the module. Winter et al. [9] envisioned PGMD as a DCMD system with in-situ cooling of the pure water stream by incoming feed water, which is preheated in the process. They note that the PGMD configuration allows for the inclusion of a more efficient energy recovery system and an additional thermal resistance in the form of the liquid gap which reduces sensible heat loss to the cold side compared to DCMD, much like the air gap in AGMD. However, the relative advantages of these two effects were not clearly identified. Another intuitive way to understand PGMD is as an AGMD system with the air gap filled completely with liquid water. Figure 1 illustrates a cross-section view of the various MD configurations investigated in this work.

Swaminathan et al. [10] extended the numerical models developed by Summers et al. [11] to study PGMD system performance. Based on these results, they also proposed a novel MD configuration, conductive gap membrane distillation (CGMD), for improved energy efficiency. In CGMD, the goal is to increase the conductivity of the gap region rather than to reduce heat conduction through the gap as in the case of AGMD. While increasing the gap conductivity would lead to an increase in undesirable heat conduction losses from the hot feed to the coolant, the overall effect is positive in terms of system level energy efficiency, expressed as a gained output ratio (GOR).

The gap conductivity can be increased by allowing the gap to be filled with water, as in the case of PGMD. In CGMD, in addition to filling the gap with water (Fig. 1), it is proposed that conductive materials be used in the region between the membrane and the plate to increase the overall thermal conductivity. Several methods of doing this, including the use of fins on the condensing surface extending up to the membrane, have been proposed.

This paper experimentally compares major single stage MD configurations including air gap (AGMD), permeate gap (PGMD), and conductive gap (CGMD) systems having the same total membrane area under similar operating conditions such as feed flow rate, external heat input and channel geometries. Various simple woven mesh spacers are used to change the thermal conductivity of the gap region to simulate CGMD conditions. These results are compared with numerical modeling results and major

trends are verified. Finally the reasons for the variation between absolute magnitudes of GOR observed in the experiments and those predicted by the model are discussed.

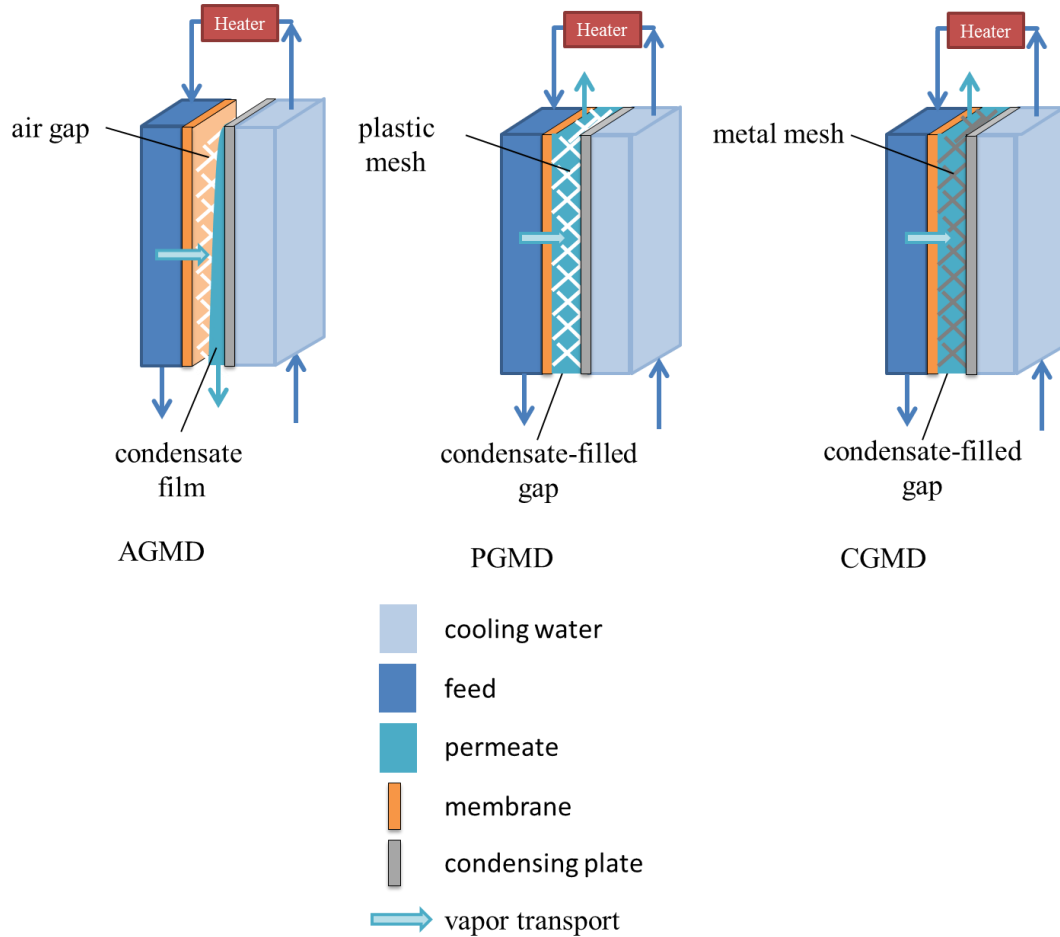


Figure 1. Membrane distillation configurations experimentally examined in this study.

II. THEORY

GOR is used in this study to quantify the efficiency of different MD systems. GOR is the non-dimensional specific pure water production rate per unit thermal power input (Eq. 1):

$$GOR = \frac{\dot{m}_p h_{fg}}{\dot{Q}_{in}} \quad (1)$$

A configuration of MD could have a higher GOR, either by producing more water under similar operating conditions or by consuming lesser thermal energy to produce a similar quantity of water. In the case of PGMD and CGMD as compared to AGMD, since the thermal resistance of the gap is reduced, the overall heat transfer coefficient between the hot side and the cold side is increased. As a result, for the same total heat exchange area (NTU), the effectiveness of heat transfer is improved and hence more heat is recovered in the preheating process within the module. This results in significant

reduction in \dot{Q}_{in} , while retaining a relatively constant value of \dot{m}_p , resulting in improved GOR. A more detailed discussion of these competing factors is presented in [10].

In order to increase the thermal conductivity of the gap, simple mesh spacers made of copper were used. The AGMD and PGMD experiments were also conducted with spacers, made of plastic, to support the membrane and prevent tearing of the membrane. Summers et al. [12] previously investigated several geometries of spacer material and found that the woven mesh spacer provided good support to the membrane. Woven mesh spacers were therefore adopted for this study as well. By choosing copper and polypropylene spacers of similar thickness, it was possible to analyze the effect of the conductivity of the spacer on GOR.

The conductance of the gap (h_{gap}) ultimately affects the MD process in PGMD and CGMD and can be expressed as

$$h_{gap} = \frac{k_{gap}}{\delta_{gap}} \quad (2)$$

where k_{gap} is the effective thermal conductivity of the gap and δ_{gap} is the thickness of the gap. The effective thermal conductivity of wire meshes in the direction perpendicular to the plane has been found to vary over a wide range of values ranging from close to 0.02 W/mK to above 100 W/mK for copper mesh in air, depending on the type of contact between the mesh elements, the geometry of the mesh, and the volumetric ratio of metal to air [13].

For the single layer copper and plastic woven meshes used in this study, without good contact (as the filaments not sintered together) between the wires, the thermal conductivity change from that of the fluid (water) is expected to be small. Rayleigh's analytical expression [14] (Eq. 3) is commonly used to estimate the effective conductivity of a single layer wire mesh in terms of the porosity (ϕ) and the conductivities of the solid (k_s) and fluid (k_f). The volumetric porosity of the mesh used is about 0.8. Under these conditions, Rayleigh's formula predicts $k_{eff,Cu,water} = 0.89$ W/mK and $k_{eff,PP,water} = 0.5$ W/mK for copper and polypropylene spacers, respectively. Thermal conductivity of water was assumed to remain constant at 0.6 W/mK.

$$k_{eff, Rayleigh} = \frac{k_f[k_w+k_s-(1-\phi)(k_f-k_s)]}{k_f+k_s+(1-\phi)(k_f-k_s)} \quad (3)$$

III. EXPERIMENTAL PROCEDURE

A schematic diagram of the experimental apparatus is shown in Fig. 2a. The feed water (0.1% NaCl solution to enable leak detection) is passed through the cold side to cool the condensing surface before being passed through a heater. The heat supply from the heater is controlled using a variable voltage controller. This heated water is then passed on the other side of the module over the MD membrane, counter-flow to the cold flow. The water is then passed back into the feed tank which is cooled to maintain it at a constant temperature. The apparatus is described in detail in Summers and Lienhard [7], with the only significant changes being reducing the channel depth to increase velocity, and adding insulation. For testing permeate gap and conductive gap configurations, further modifications were made.

In the above apparatus, the gap between the MD membrane and the condensing surface was modified to conduct experiments on AGMD, PGMD, and CGMD configurations. For AGMD, a plastic woven mesh is used. For PGMD, the same plastic woven mesh is used to support the mesh while water is now collected from the top with the bottom sealed so that the gap gets filled with liquid water (Fig. 2b). In the case of CGMD, in addition to collecting water from the top, the plastic mesh is replaced by a metal mesh.

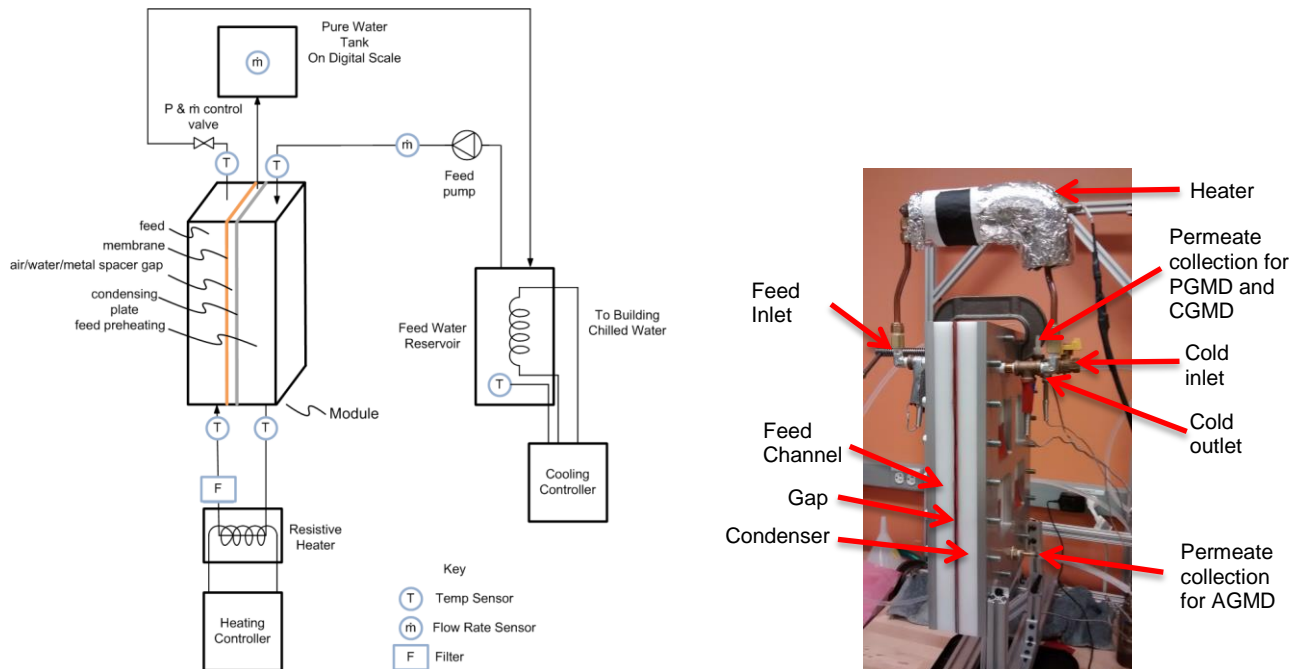


Figure 2. Left: Schematic diagram of experimental system. Right: Photograph of MD module

During operation, fiberglass insulation was used on the inlets and exits to the heater, and foam insulation was applied on the outer surface to reduce the heat loss to the environment. The feed stream is circulated using a magnetic drive pump with no metallic parts exposed to the fluid. Low mass flow rate was achieved using the needle valve at the outlet of the module just before the flow returns to the tank. Therefore most of the pressure drop occurs after the feed stream leaves the MD module. This keeps the static pressure inside the module high enough to maintain a flat membrane. Feed flow rate was measured by collecting the feed for a known time interval (e.g., 50 sec.) and measuring its weight using a scale with 0.01 g accuracy. Permeate flow rate was calculated in a similar manner. Temperatures were measured using type T thermocouples with 1 °C accuracy. A cloth filter was used following the heater before flow entered the hot side of the MD module to prevent rust particulates from the heater depositing on the membranes and leading to membrane wetting.

Experiments were carried out under the same heater energy input conditions while varying the feed mass flow rate for each configuration, with different mesh sizes in the gap.

IV. RESULTS

Numerical models for the different MD configurations has been developed by the authors and described in detail in [10]. While the air gap was modeled as shown in [11], for the permeate gap and the conductive gap configurations the flow of pure water through the gap is neglected and the heat transfer through the gap is approximated as conduction between the membrane and condensing surface. The total length of the channel is 0.85 m, the width is 0.05 m, and the channel depth is 0.035 m. The channels are arranged such that the hot and cold fluid streams are in a counterflow orientation. The simulations were conducted at a constant power input of 90 W. The effective conductivity of the permeate gap is set as 0.6 W/mK, whereas for the conductive gap case, an effective conductivity of 10 W/mK is used. These would refer to the best case scenario values for k_{gap} . As highlighted earlier, with the simple woven meshes, the conductivity in the permeate gap experiments is likely to be approximately 0.5 W/mK, and about 0.9 W/mK rather than 10 W/mK in the copper mesh CGMD experiments. These results are then compared with the best-case scenarios to determine the trends and evaluate how much further improvement is possible.

Figure 3(a) shows the numerical modeling prediction on the effect of gap thermal conductivity on GOR. At lower values of k_{gap} , up to about 4 W/mK, a steep increase in GOR is predicted, followed by diminishing returns beyond this point. The exact number is a function of the relative dominance of the gap resistance among other thermal resistances between the hot and cold fluids. One can observe that an ideal CGMD process should have about twice as much GOR as that of AGMD, when all other parameters are held constant.

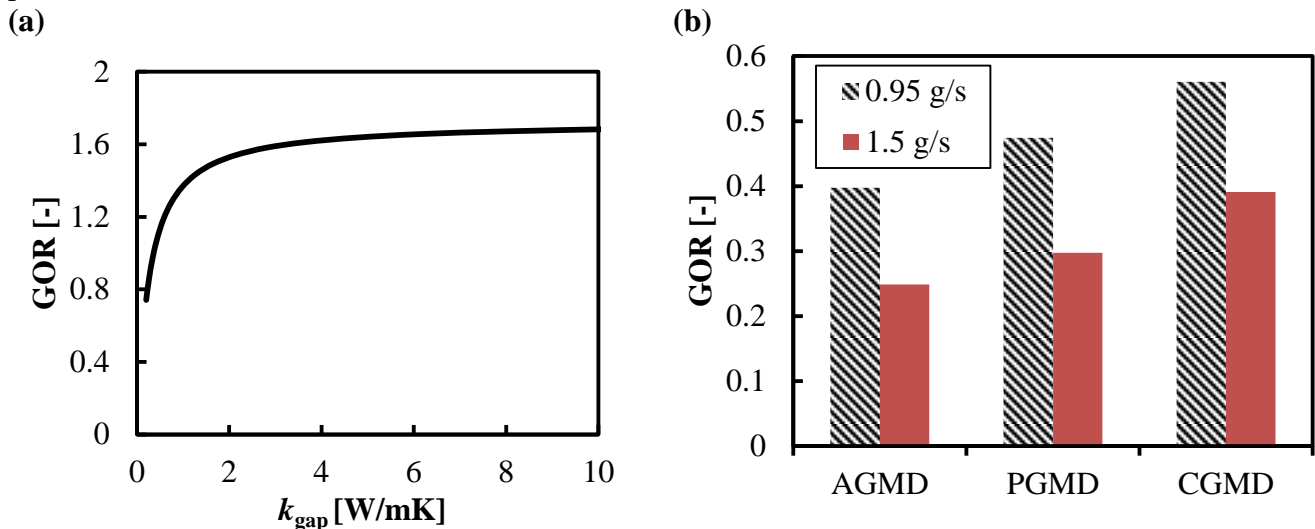


Figure 3. (a) Numerical model results on effect of k_{gap} on GOR ($\dot{m}_f = 1$ g/s, $d_{gap} = 1.24$ mm). (b) Experimental GOR at $d_{gap} = 1.24$ mm for different MD configurations and two feed flow rates.

Figure 3(b) shows experimental results on the effect of gap configuration on GOR at two values of feed flow rate. Under both flow rate conditions, an increasing trend of GOR is observed between the AGMD, PGMD, and CGMD configurations. The magnitude of increase in GOR between AGMD and CGMD is between 40 to 60%, whereas between AGMD and PGMD it is about 20%. The flux at a GOR of 0.3 is 2.43 LMH. The heat supply rate was held constant at 174 W in all the experiments and so the GOR is a linear function of the flux.

As noted in Section III, another method to affect the process performance by changing gap conductance is to change d_{gap} . Figure 4a shows that lower d_{gap} leads to a higher GOR for all configurations. In the case of CGMD, the improvement is less pronounced as the increase in h_{gap} does not affect the total resistance much because of the aforementioned diminishing returns, as the gap is no longer a major resistance. It should be noted that this figure indicates that while AGMD and PGMD perform worse at higher d_{gap} , at lower gap thicknesses their performance approaches that of CGMD. Practical constraints such as the pressure drop for the permeate flow will set the lower limit on d_{gap} in these cases.

Experimentally, mesh thickness effectively sets the gap thickness. Energy efficiency using a mesh thickness of 1.12 mm was found to be higher than using a 1.24 mm thick mesh. As predicted by the model, the improvement in GOR is higher for AGMD than for PGMD, 23% compared to 12%, while the magnitudes of GOR in the PGMD case are higher.

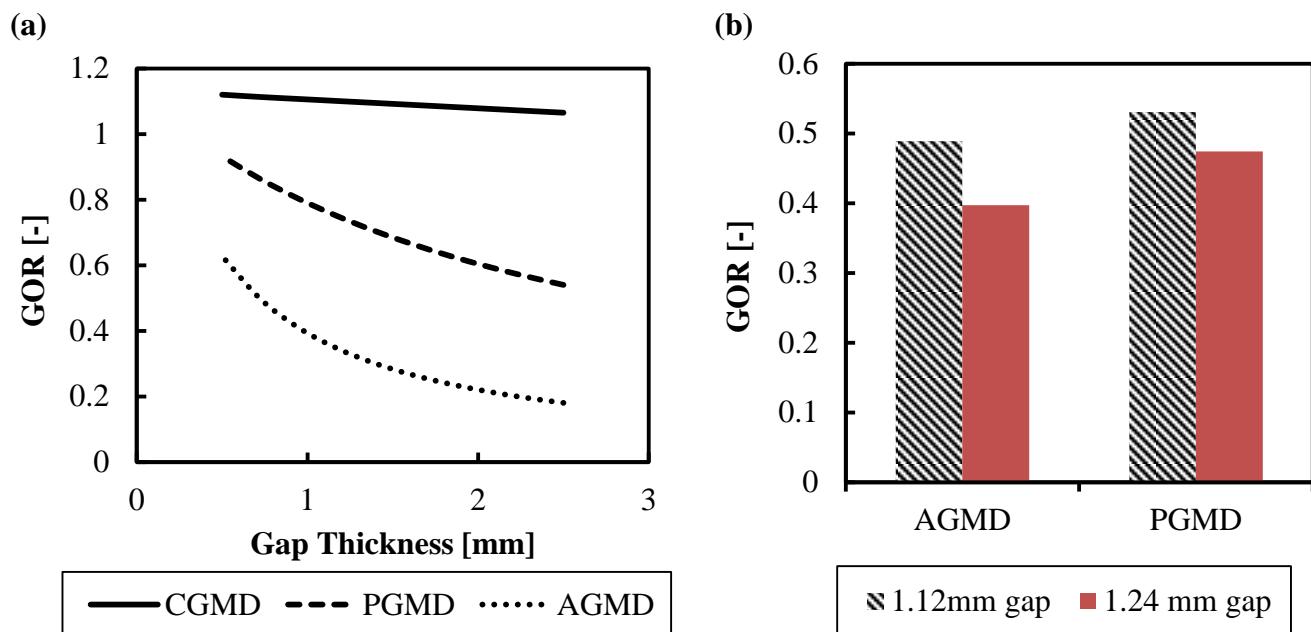


Figure 4. (a) Numerical modeling predictions on the effect of gap thickness on GOR ($\dot{m}_f = 1.5 \text{ g/s}$). (b) Experimental results on the effect of gap thickness on AGMD, PGMD performance at $\dot{m}_f = 0.95 \text{ g/s}$.

Figure 5(a) shows numerical modeling results on the effect of feed flow rate on GOR. In all three configurations, a smaller feed flow rate leads to a higher GOR due to better energy regeneration in the MD module (larger NTU for the same area and transfer coefficient). Also the GOR increases exponentially as we get to very small flow rates, and is limited only by the increase in flow boundary layer resistances to heat and mass transfer.

Experimentally, a similar trend is observed in terms of the effect of feed flow rate (Fig. 5(b)). At lower feed mass flow rates, for the same external heat input, the feed stream is heated more as it leaves the cold channel leading to higher top temperature and higher water permeate production rate. The reason why CGMD performs better at any given flow rate is also similar. For the same set of inlet conditions

and heat input, the CGMD system has better internal heat transfer coefficients, enabling more heat transfer in the module leading to better preheating of the cold stream. As a result, the cold outlet stream temperature is higher in CGMD compared to PGMD which in turn is higher than AGMD. Since the heat input is constant, this leads to a higher top temperature in CGMD and therefore higher flux and pure water production rates. This experimentally observed mechanism is also numerically verified.

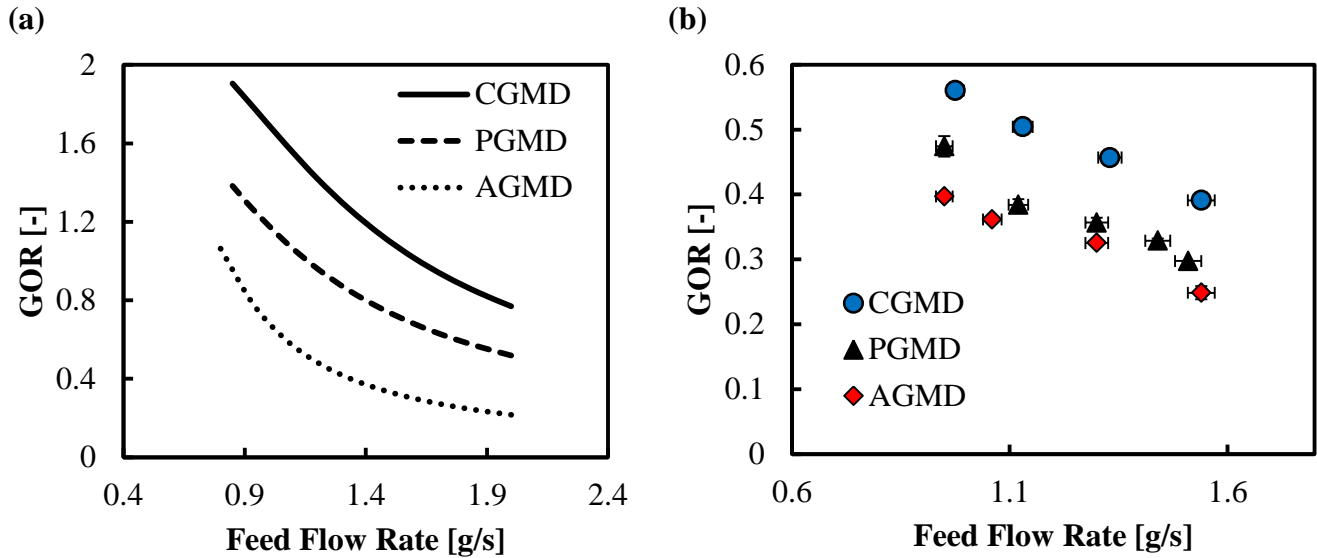


Figure 5. (a) Numerical model predictions on GOR as a function of feed flow rate. (b) Experimental GOR as a function of flow rate, $d_{\text{gap}} = 1.24$ mm

V. DISCUSSION

While the results in Section IV are consistent with those from the numerical model, on average the absolute magnitude of the numerically predicted GORs is about twice that of the experimentally observed GORs. This section discusses some of the reasons for this mismatch and suggestions for future bench scale MD energy efficiency experiments.

The two major reasons for the mismatch between experiments and the model are heat losses to the environment, which are neglected in the model, and cross-conductance in the condensing plate due to compact module design. In addition to these, the reason for the relative improvement in CGMD performance in the experiment being lower than that predicted numerically has been explained briefly in terms of the actual effective thermal conductivity of the mesh spacer used for CGMD being much below the value of 10 W/mK assumed in the model.

5.1 Compact MD modules and cross-conductance

For MD installations of small membrane area, the feed flow rate needs to be low as described in Section IV. This can be understood based on the fact that MD flux is likely to be about 2-4 L/m²hr for a well-designed system with energy recovery. As a result, for smaller membrane area systems, the feed flow rate needs to be scaled down in order to achieve a good recovery ratio in the module.

Lower feed and coolant flow rates lead to higher temperature and concentration polarization in these channels. In order to accommodate a longer channel within the feed and cold side plates, circuitous flow geometry was used, as shown in Fig. 6. This leads to cross conduction in the copper condensing plate leading to the MD module's departure from counter-flow behavior thereby degrading heat recovery substantially.



Figure 6: Flow channel geometry.

5.2 Heat loss

In the numerical model, heat loss to the environment was neglected. The channel was machined out of Delrin plates of 2.54 mm thickness to provide insulation. In addition, insulation was used, but couldn't cover the module uniformly. The heat loss to the environment scales as $\dot{Q}_{loss} = h_{eff}A_s\Delta T_{eff}$ where h_{eff} and ΔT_{eff} are effective heat transfer coefficient and temperature difference associated with the heat loss. The effective heat transfer coefficient is the effective conductance of a series network of forced convection, conduction through module housing and natural convection resistances. In most cases, natural convection resistance is the dominant resistance. For the range of experimental conditions, natural convection heat transfer coefficient is proportional to ΔT_{eff} to a power less than one (e.g., 1/6). Therefore, h_{eff} can be considered to be approximately constant. In the current experiments, same amount of heat input was used. The feed stream is heated up to a higher temperature when the mass flow rate is lower. So at lower mass flow rate, ΔT_{eff} is higher, resulting in an increased heat loss. In this experimental setup, heat loss was significant, accounting for roughly 20% of the heater power. Again, for lower mass flow rates, the heater power as an absolute magnitude is lower. While \dot{Q}_{loss} is a function of only the surface area and ΔT_{eff} , and is not directly affected by changes in flow rate, for a constant top temperature system for example, the magnitude of heat input would still be lower for the lower mass flow rate system, leading to a higher percentage heat loss. This large heat loss is the second reason why GOR was low for this experimental setup. While the numerical model ignores heat loss and predicts an exponential increase in GOR, at lower flow rates the experiment shows a leveling off of GOR. This too is a result of higher heat losses at the lower flow rate cases due to higher top temperature in the module, as shown in Fig. 7. The heat loss is calculated by applying the energy balance on the MD module as shown in Eq. 4.

$$\dot{Q}_{loss} = \dot{m}_f c_p T_h - \dot{m}_b c_p T_h - \dot{m}_p c_p T_p + \dot{m}_f c_p (T_{c,in} - T_{c,out}) \quad (4)$$

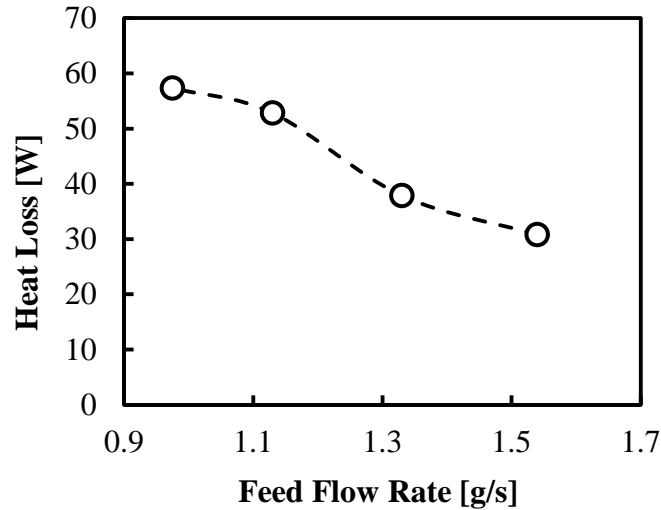


Figure 7: Heat loss as function of feed mass flow rate for CGMD (1.24 mm copper mesh) test with 174 W total heat input

VI. CONCLUSIONS

Numerical models predict that the GOR of a well-designed CGMD configuration with high k_{gap} can be more than two times higher than that of an AGMD system of the same membrane area. Experimentally, using woven mesh spacers of relatively low k_{eff} , the predicted trends in GOR were verified. The CGMD system GOR was up to 60% higher than that of AGMD, and PGMD outperforms AGMD by about 20%. The higher GORs of PGMD and CGMD are due to lower transport resistances within the module leading to better preheating of the feed. The effect on reducing flux of heat loss and cross-conductance in MD modules machined compactly with common condensation surface is explained, which may facilitate better design of future bench-scale conductive-gap MD experiments for studying GOR.

VII. ACKNOWLEDGEMENT

This work was funded by the Cooperative Agreement Between the Masdar Institute of Science and Technology (Masdar Institute), Abu Dhabi, UAE and the Massachusetts Institute of Technology (MIT), Cambridge, MA, USA, Reference No. 02/MI/MI/CP/11/07633/GEN/G/00, and facilitated by the MIT Deshpande Center for Technological Innovation and the Masdar Institute Center for Innovation and Entrepreneurship (iInnovation). We acknowledge Ann McCall Huston, Grace Connors and Priyanka Chatterjee for assisting with the experiments.

VII. REFERENCES

- [1] E. Curcio and E. Drioli, "Separation & Purification Reviews Membrane Distillation and Related Operations – A Review," *Separation and Purification Reviews*, vol. 34, pp. 35–86, 2005.

- [2] M. Khayet, “Membranes and theoretical modeling of membrane distillation: A review,” *Advances in Colloid and Interface Science*, vol. 164, no. 1-2, pp. 56–88, 2011.
- [3] E. K. Summers and J. H. Lienhard V, “A novel solar-driven air gap membrane distillation system,” *Desalination and Water Treatment*, vol. 51, pp. 1–8, 2012.
- [4] K. Zhao, W. Heinzl, M. Wenzel, S. Büttner, F. Bollen, G. Lange, S. Heinzl, and N. Sarda, “Experimental study of the memsys vacuum-multi-effect-membrane-distillation (V-MEMD) module,” *Desalination*, vol. 323, pp. 150–160, 2013.
- [5] J. Gilron, L. Song, and K. K. Sirkar, “Design for cascade of crossflow direct contact membrane distillation,” *Industrial & Engineering Chemistry Research*, vol. 46, no. 8, pp. 2324–2334, 2007.
- [6] F. He, J. Gilron, and K. K. Sirkar, “High water recovery in direct contact membrane distillation using a series of cascades,” *Desalination*, vol. 323, pp. 48–54, 2013.
- [7] E. K. Summers and J. H. Lienhard V, “Experimental study of thermal performance in air gap membrane distillation systems including direct solar heating of membranes,” *Desalination*, vol. 330, pp. 100–110, 2013.
- [8] J. Swaminathan and J. H. Lienhard V, “Energy efficiency of sweeping gas membrane distillation desalination cycles,” in *Proceedings of the 22nd National and 11th International ISHMT-ASME Heat and Mass Transfer Conference, IIT Kharagpur, India 2014*, Dec. 2014.
- [9] D. Winter, J. Koschikowski, and M. Wieghaus, “Desalination using membrane distillation: Experimental studies on full scale spiral wound modules,” *Journal of Membrane Science*, vol. 375, no. 1, pp. 104–112, 2011.
- [10] J. Swaminathan, D. Warsinger, H. W. Chung, and J. H. Lienhard V, “Conductive gap membrane distillation for energy efficient desalination,” *in preparation*, March 2015.
- [11] E. K. Summers, H. A. Arafat, and J. H. Lienhard V, “Energy efficiency comparison of single-stage membrane distillation (MD) desalination cycles in different configurations,” *Desalination*, vol. 290, pp. 54–66, 2012.
- [12] E. K. Summers, *Development of Energy Efficient Membrane Distillation Systems*. PhD thesis, Massachusetts Institute of Technology, Cambridge, Massachusetts, U.S.A., 2013.
- [13] C. Li and G. Peterson, “The effective thermal conductivity of wire screen,” *International Journal of Heat and Mass Transfer*, vol. 49, no. 21, pp. 4095–4105, 2006.
- [14] L. Rayleigh, “On the influence of obstacles arranged in rectangular order upon the properties of a medium,” *The London, Edinburgh, and Dublin Philosophical Magazine and Journal of Science*, vol. 34, no. 211, pp. 481–502, 1892.

